01,07

Elastic Properties of B2-NiAl with W addition: A first-principles study

© A.V. Ponomareva

Materials Modeling and Development Laboratory
National University of Science and Technology „MISIS“
Moscow, Russia

Email: alena.ponomareva@misis.ru

Received September 15, 2022
Revised September 15, 2022
Accepted September 16, 2022

The effect of tungsten alloying on the elastic properties of B2-NiAl at low-temperature and high-temperature distribution of W atoms on sublattices. By means of the exact muffin-tin orbitals method in conjunction with the coherent potential approximation, the constants C_{11}, C_{12}, C_{44}, Young's modulus E, shear modulus G, Cauchy pressure values, G/B ratios are calculated. Using phenomenological criteria of the correlation between ductility and elastic properties of solution phases, it has been shown that the addition of tungsten could yield improved ductility for B2-NiAl in both types of alloys. It is established that with the high-temperature distribution of W atoms on the Al sublattice, there is a loss of mechanical stability and a decrease in mechanical properties with increasing W concentration. In alloys with a low-temperature distribution of tungsten atoms between Al and Ni sites a unique combination of properties occurs: in addition to the ductility enhancement, a simultaneous increase of the elastic constants C_{44} and C_{11} and C_{11}, shear modulus G, Young's modulus E with increasing W content is observed. The differences in the behavior of elastic constants in alloys with different types of tungsten distribution on NiAl sublattices are analyzed by calculating the density of electronic states.

Keywords: NiAl, alloying elements, tungsten, elastic properties, ductility, first-principles calculations.

DOI: 10.21883/PSS.2023.01.54968.477

1. Introduction

NiAl-based alloys with a cubic structure of B2 are widely used in various industries due to a number of outstanding properties. High melting point, wide area of homogeneity, high thermal conductivity, low density allow the use of materials based on B2-NiAl in aircraft and rocket engineering, electronics. Due to the high anti-corrosion properties and excellent performance at high temperatures and pressures, nickel-based alloys are used in modern nuclear power systems [1]. One of the limiting factors in the use of B2-NiAl is low plasticity in the coarse-crystalline state, lack of crack resistance at room and low temperatures, as well as insufficient strength at temperatures above 1100° K. Embrittlement of these alloys can be reduced in several ways, including micro- and macroalloying. Thus, in the study [2] it is reported that grinding grain to nanometric sizes in NiAl-based alloys improves their plastic characteristics. In a number of studies, it was possible to achieve an increase in plasticity due to the formation of a specific microstructure, for example, the formation of fibers and reinforcement of the second phase by adding Mo, Fe, Cr, Co, W, Hf, Ti [3–5], as well as inclusions of borides and carbides of molybdenum and tungsten [6,7] or carbon nanotubes [8]. The authors of the study [9] managed to increase the plasticity of aluminum nickelide as a result of fusion with lanthanum due to partial disordering of the atomic structure. The theoretical studies [10–13] structural, electronic and elastic properties of NiAl with alloying elements have shown that Cr, Mo, Tc, Ru, Rh and Pd are promising candidates for improving the mechanical properties of aluminum nickelide.

Previously, we investigated the effect of alloying Sc, Ti, Cr, Co, V, W, Re on the elastic properties of B2-NiAl alloys under the condition of an energetically favorable arrangement of the third element along the sublattices at $T = 0\,\mathrm{K}$ [14–16]. The main result of [14] is the calculation of the elastic characteristics of the materials under study — elastic constants C_{11}, C_{12}, C_{44}, volume modulus B, Young's modules E and shift G, anisotropy coefficients. Elastic constants are important characteristics of structural alloys and are used to assess the mechanical stability and strength characteristics of materials. Calculations have shown that the additives W, V, Re and Ti can improve the ductility of B2-NiAl without significantly changing the macroscopic elastic modulus. In [15], a detailed study of the effects of fusion of NiAl with Re was performed, the concentration behavior of elastic characteristics and their relationship with the interatomic interaction were investigated. In the work [16], the burning synthesis was used to experimentally confirm the results of modeling the effects of Ti alloying on the properties of B2-NiAl. It is shown that the experimental value of the Young's modulus synthesized $(Ti_{50}Al_{50})Ni$ alloy, obtained by the microindentation method, agrees very well with the theoretical calculation, confirming the reliability of theoretical research methods.

In this paper we investigate in detail the influence of W on elastic characteristics B2-NiAl. Despite the fact that the solubility of tungsten in NiAl by the metallurgical method is very low, the production of alloys by other methods, for example, deposition, mechanical fusion, self-propagating high-temperature synthesis, aluminothermic reduction of metal oxides can achieve significantly greater solubility. As we have shown in the work [14] in the study of the so-called transfer energy, which allows us to take into account the possibility of the formation of an antistructural defect, at $T = 0$ K atoms W occupy positions on both Al and Ni sublattices. This coincides with the results of the work [17], in which it is shown that at low temperatures the atoms W are located on both sublattices simultaneously, however, at higher temperatures they show preference for the Al sublattice. Therefore, we have considered the effect of tungsten alloying on the elastic properties of B2-NiAl with low-temperature and high-temperature methods of placing W on sublattices.

2. Calculation details

The elastic constants Ni–Al–W of alloys were determined based on the calculation of the total energies of deformed lattices, while the deformation retained the volume of the original, undeformed lattice in the domain of Hooke's law [18]. For cubic crystals, there are three independent elements of the tensor of elastic constants: C_{11}, C_{12}, C_{44}.

The constants C_{11} and C_{12} are determined from the relations

$$C_{11} = 3B + 4C'/3, \tag{1}$$

$$C_{12} = 3B - 2C'/3, \tag{2}$$

where B is the bulk modulus, C' is the tetragonal shift modulus. The bulk modulus B was obtained from the calculation of the equation of state.

The elastic constant C' was obtained using an orthorhombic deformation of the form

$$I + D_0 = \begin{pmatrix} 1+\delta & 0 & 0 \\ 0 & 1-\delta & 0 \\ 0 & 0 & 1/1-\delta^2 \end{pmatrix}, \tag{3}$$

as the coefficient of the corresponding change in energy from the square of the deformation:

$$\Delta E/V = 2C'\delta^2 + O(\delta^4). \tag{4}$$

The constant C_{44} was calculated using monoclinic distortion

$$I + D_M = \begin{pmatrix} 1 & \delta & 0 \\ \delta & 1 & 0 \\ 0 & 0 & 1/1-\delta^2 \end{pmatrix} \tag{5}$$

and the change in total energy

$$\Delta E/V = 2C_{44}\delta^2 + O(\delta^4). \tag{6}$$

The total energy was calculated for six different deformations ($\delta = 0.00–0.05$), then the elastic constants C' and C_{44} were determined using the linear approximation ΔE as a function of the square of the deformation. Further, using the values of the volume modulus, the elastic constants C_{11} and C_{12} were determined from equations (1) and (2).

The stability criterion of the crystal lattice is obtained from the condition that the energy density can be represented by a positive definite quadratic form in such a way that the energy increases with any small deformation. Therefore, all diagonal components of the tensor of elastic constants must have positive values. Therefore, for cubic crystals, the stability criterion is determined by the expressions

$$C_{44} > 0, \quad C_{11} - C_{12} > 0, \quad C_{11} + 2C_{12} > 0. \tag{7}$$

To obtain the elastic characteristics of polycrystals, averaging over Hill (H) [19,20] was used. The values of the characteristics in the Hill approximation are the arithmetic mean of the values obtained in the Reuss (R) and Voigt (V) [19] approximations.

The first method corresponds to the assumption of uniformity of deformations in a polycrystal, the second — uniformity of stresses, and the obtained values of elastic characteristics give the upper and lower limits of the change in the corresponding properties [19].

For cubic crystals we have

$$B_R = B_V = (C_{11} + 2C_{12})/3, \tag{8}$$

$$G_V = (C_{11} - C_{12} + 3C_{44})/5, \tag{9}$$

$$G_R = \big(5C_{44}(C_{11} - C_{12})\big)/\big(4C_{44} + 3(C_{11} - C_{12})\big), \tag{10}$$

$$E = 9BG/(3B + G). \tag{11}$$

Parameters such as Cauchy pressure $P_C = (C_{12}–C_{44})$ [21] and the ratio (G/B) [22], were used to analyze changes in phenomenological ratios as a result of alloying, which can be considered as indicators of the brittleness of materials. For covalent materials with directional atomic bonds, the Cauchy pressure is negative ($C_{12} < C_{44}$), since in this case the material's resistance to shear deformation (C_{44}) is significantly greater than for volume changes (C_{12}). On the other hand, for metallic bonds where the electrons are almost delocalized, the Cauchy pressure must be positive ($C_{12} > C_{44}$). The ratio G/B can also be considered as a measure of ductility [22]. The bulk modulus B is associated with the resistance to change in the bond length, and the shear modulus G corresponds to a change in the bond angle. Therefore, if $G/B < 0.5$, then the material behaves in a ductile manner, if $G/B > 0.5$, then the material must be brittle.

Calculations were carried out using the method of exact MT-orbitlei (EMTO) [18] and the approximation of the coherent potential (CPA) [23]. The EMTO method combination with the approximation of the coherent potential

made it possible to conduct studies of disordered and partially disordered W-NiAl alloys. In the EMTO method, the total non-spherical charge density, and then kinetic energy, is obtained by an exact self-consistent solution of the one-electron Kohn–Shem equation for overlapping MT potentials. This makes it possible to achieve accuracy comparable to full-potential methods, while maintaining the effectiveness of methods based on the use of MT-potentials [24–28].

The exchange-correlation effects in the electron gas were taken into account in the framework of the generalized gradient approximation (GGA) [29]. The basic set of EMTO wave functions included s-, p-, d-, f-orbitals. The full charge density (FCD) [30] was represented by a one-center decomposition of electronic wave functions in terms of spherical harmonics with orbital moments $l_{\mathrm{FCD}}^{\max} = 8$. Energy integration was carried out at 24 points on a semicircular contour. To calculate elastic properties, integration over the irreducible part of the Brillouin zone was carried out using the grid $31 \times 31 \times 31$ k-points in the inverse space. The convergence of the energy with respect to the calculation parameters was 10^{-7} Ry.

3. Results and discussion

To study the effect of alloying W, the elastic constants C_{11}, C_{12}, C_{44}, Young's modulus E and shear modulus G of triple NiAl-W were determined for the elastic properties of B2-NiAl alloys. We note that for B2-NiAl, a good agreement was found between the theoretical and experimental lattice parameter, volume modulus, elastic constants (Fig. 1 and Ref [14]). Fig. 1 shows the elastic properties $W_xAl_{50-x/2}Ni_{50-x/2}$ of alloys with low-temperature distribution of tungsten atoms over the sublattices Al and Ni, and $W_xAl_{50-x}Ni_{50}$ alloys with high-temperature placement of W atoms on an aluminum sublattice (we note that in the case of high-temperature placement, x denotes the concentration on the sublattice, i.e. the total concentration of W in the alloy is $x/2$). It can be seen from Fig. 1 that $W_xAl_{50-x/2}Ni_{50-x/2}$ alloys in which tungsten atoms are placed on both sublattices are stable over the entire concentration range, since all criteria for the mechanical stability of cubic crystals represented by equations (7). At the same time, for $W_xAl_{50-x}Ni_{50}$ alloys in which the atoms W are placed only on the sublattice Al, the curves C_{11} and C_{12} intersect at the point $x \sim 30$, so the criterion of mechanical stability $(C_{11}-C_{12}) > 0$ is executed only at $x < 30$.

At low concentrations of tungsten, the behavior of the elastic constants C_{11} and C_{12} is almost the same for both types of alloys: C_{11} to $x \sim 10$ almost does not change, and C_{12} starts to increase. With a further increase in the tungsten content, C_{11} and C_{12} for disordered $W_xAl_{50-x/2}Ni_{50-x/2}$ alloys increase, for partially disordered $W_xAl_{50-x}Ni_{50}$ alloys C_{12} also increases, and C_{11} — decreases with W concentration. At the same time, there are differences in the behavior of the values of the shift constant C_{44}, the Young's modulus E and the shift modulus G with different distribution of tungsten over sublattices: in $W_xAl_{50-x}Ni_{50}$ alloys C_{44}, G and E decrease, while in $W_xAl_{50-x/2}Ni_{50-x/2}$ alloys all these the parameters increase, with the maximum change in the elastic constant C_{44}. The bulk modulus B increases with the concentration of tungsten for both types of alloys, the maximum increase is observed for $W_xAl_{50-x}Ni_{50}$ alloys.

Phenomenological correlations between ductility and elastic constants were analyzed using the Cauchy pressure values $(P_C = C_{12}-C_{44})$ and the ratio G/B. As it was shown in [14], B2-NiAl has a mixed covalent-metallic type of bond with the presence of an ionic component and is quite close to the boundary of G/B brittle materials, which is confirmed by experimental data (Fig. 1). The change of P_C and G/B depending on the concentration of W indicates the possibility of improving ductile properties, i.e. the value of the ratio G/B decreases, and the values P_C — increases. At the same time, in $W_xAl_{50-x}Ni_{50}$ alloys, the changes in the brittleness parameters are more significant than in $W_xAl_{50-x/2}Ni_{50-x/2}$ alloys. In $W_xAl_{50-x}Ni_{50}$ alloys, we limited the dependence of the elastic characteristics of $E, G, G/B$ to the concentration of tungsten $x = 30$, since when the region of mechanical instability is reached, the Reuss approximation, which gives a contribution to the Hill approximation used becomes unacceptable, since it uses the uniform deformation mode [19]. As can be seen from the formulas (10) and (11) in the Reuss approximation, the modules G and E are proportional to $(C_{11}-C_{12})$, therefore, at $x > 30$, they show nonlinear behavior with a departure in negative area.

Thus, the different placement of tungsten along the sublattices leads to significant differences in the properties of alloyed aluminum nickelide: with loss of mechanical stability by $C' = (C_{11}-C_{12})/2$ at high temperature arrangement and with an increase in elastic characteristics and ductility at low-temperature placement.

In order to understand the reason for the different behavior of elastic characteristics in the studied systems, the change in the density of electronic states (DOS) during alloying was analyzed in detail (Fig. 2). At low concentrations of tungsten, the total density of states almost retains the DOS form of pure NiAl (Fig. 2, $a1-a3$), in which the main contribution to DOS in the Fermi energy region is made by a narrow d-band Ni. It consists of so-called non-bonding (the main contribution from t_{2g} electrons with a small contribution of e_g electrons) and anti-bonding (e_g) states separated by a pseudo-gap. A detailed description of DOS pure B2-NiAl is given in the article [14]. The difference in the total density of states in $W_xAl_{50-x}Ni_{50}$ and $W_xAl_{50-x/2}Ni_{50-x/2}$ alloys at $x = 10$ (Fig. 2, $a1$) are minimal: a slight blurring of peaks and a slight shift to the right of the full DOS due to a decrease in the concentration of Ni in $W_xAl_{50-x/2}Ni_{50-x/2}$alloys compared to $W_xAl_{50-x}Ni_{50}$ alloys. However, the partial density shows the main difference between the alloys: in $W_xAl_{50-x/2}Ni_{50-x/2}$, a peak of t_{2g} states of W(Ni) appears (tungsten located on

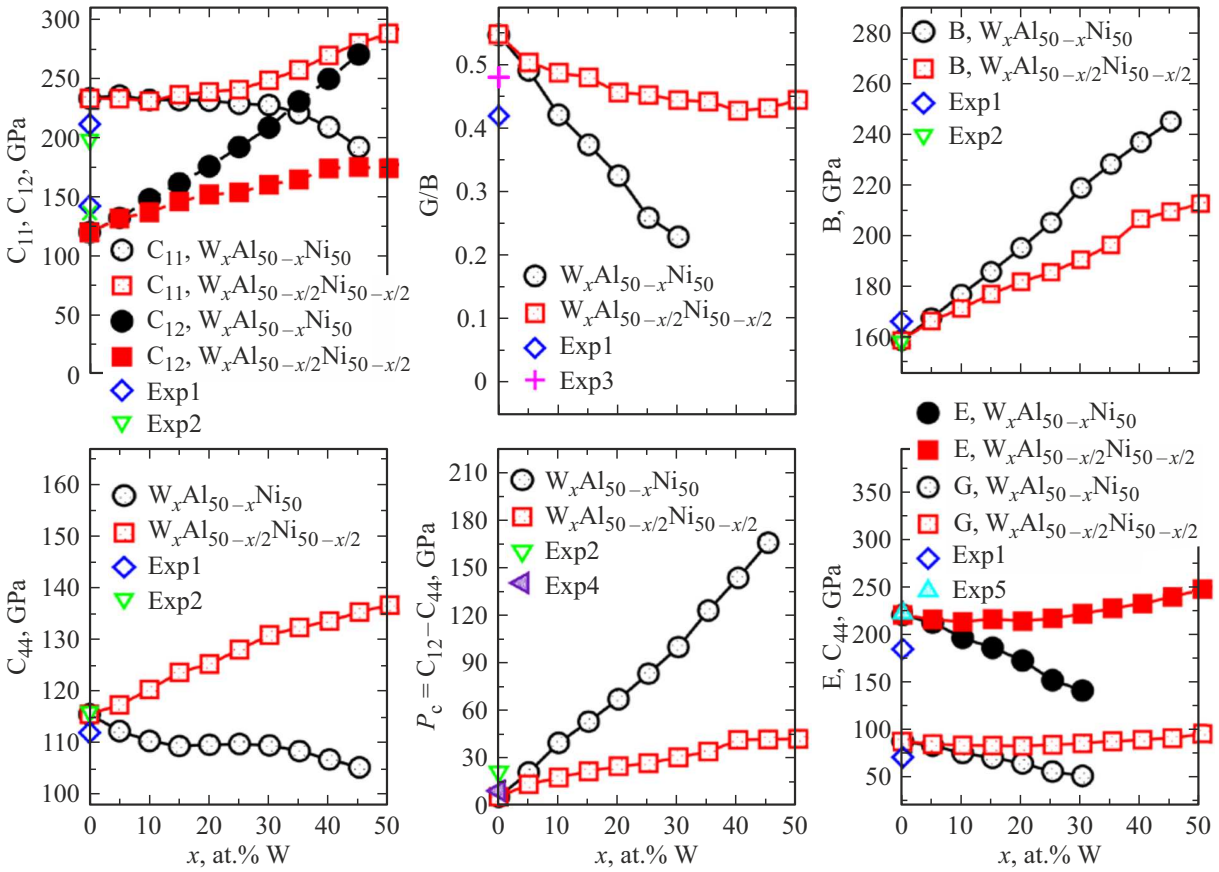

Figure 1. Elastic constants C_{11}, C_{12}, C_{44}, ratio G/B, the Cauchy pressure $P_C = (C_{12} - C_{44})$, volume modules B, shear modules G and Young's modules E of $W_xAl_{50-x/2}Ni_{50-x/2}$ and $W_xAl_{50-x}Ni_{50}$ alloys. The figure uses notation for experimental data: Exp1 — [31], Exp2 — [32], Exp3 — [33], Exp4 — [34], Exp5 – [15].

a nickel sublattice) (Fig. 2, *e*1, green line), which is shifted towards the Fermi energy relative to the t_{2g} states of W(Al) (tungsten located on an aluminum sublattice) (Fig. 2, *e*1, black line). Since t_{2g} orbitals in BCC-type structures provide an interatomic bond between the first neighbors, then this effect provides an increase in $sp-d$-hybridization between electrons W and Al (Fig. 2, *e*1–*e*3), which leads to an increase in the shear constants C_{44} in $W_xAl_{50-x/2}Ni_{50-x/2}$ alloys (Fig. 1).

In alloys $W_xAl_{50-x}Ni_{50}$, there are no W(Ni) states, since tungsten atoms are located only on the aluminum sublattice, moreover, t_{2g} states W(Al) has a low DOS, and e_g zero density of states in the energy range $-0.2 - -0.05$ Ry (Fig. 2, *d*1–*d*3), therefore, when placing tungsten on the aluminum sublattice, the bond with Ni atoms decreases, and with Al atoms. This leads to a simultaneous decrease in the elastic constants C_{11} and C_{44}, as well as the modules G and E in $W_xAl_{50-x}Ni_{50}$ alloys (fig. 1).

With an increase in the concentration of tungsten on the nickel sublattice, the proportion of e_g states W(Ni) with a nonzero density of states in the range $-0.2 - -0.1$ eV appears and grows (Fig. 2, *e*1–*e*3), which leads to an increase in the elastic constant C_{11} and a slight increase in the shear modulus G and Young's modulus E in $W_xAl_{50-x/2}Ni_{50-x/2}$ alloys at $x > 20$. An increase in the elastic constant C_{11} in $W_xAl_{50-x/2}Ni_{50-x/2}$ alloys also occurs due to refilling of the aluminum band with 5*d* electrons W, having a large spatial extent. At the same time, due to the tails of 5*d* electrons W, the size of the pseudo-gaps decreases, the total density of states $W_xAl_{50-x/2}Ni_{50-x/2}$ alloys becomes smoother in the Fermi energy region (Fig. 2, *f*1–*f*3).

As follows from Fig. 1, in alloys with both ways of placing tungsten, the ratio of G/B decreases, and P_C becomes more positive with an increase in the concentration of tungsten, which indicates an increase in the metal fraction in the atomic bond. This is, firstly, caused by the blurring of the peaks of both Ni and W (Fig. 2, *c*1–*c*3, *d*1–*d*3) because of disorder on one or both sublattices. Secondly, there is a redistribution of nickel electrons between t_{2g}- and e_g-orbitals: the peaks of t_{2g} decrease and blur, while e_g peaks fill up and shift towards lower energy. This effect is more pronounced in $W_xAl_{50-x}Ni_{50}$ alloys, since their nickel concentration is higher than in $W_xAl_{50-x/2}Ni_{50-x/2}$ alloys. Thus, an increase in the uniformity of the electron density $(t_{2g} + e_g)$ additionally strengthens the metallic bond in $W_xAl_{50-x}Ni_{50}$ alloys. On the other hand, the loss of the coupling directivity leads to an increase in the resistance

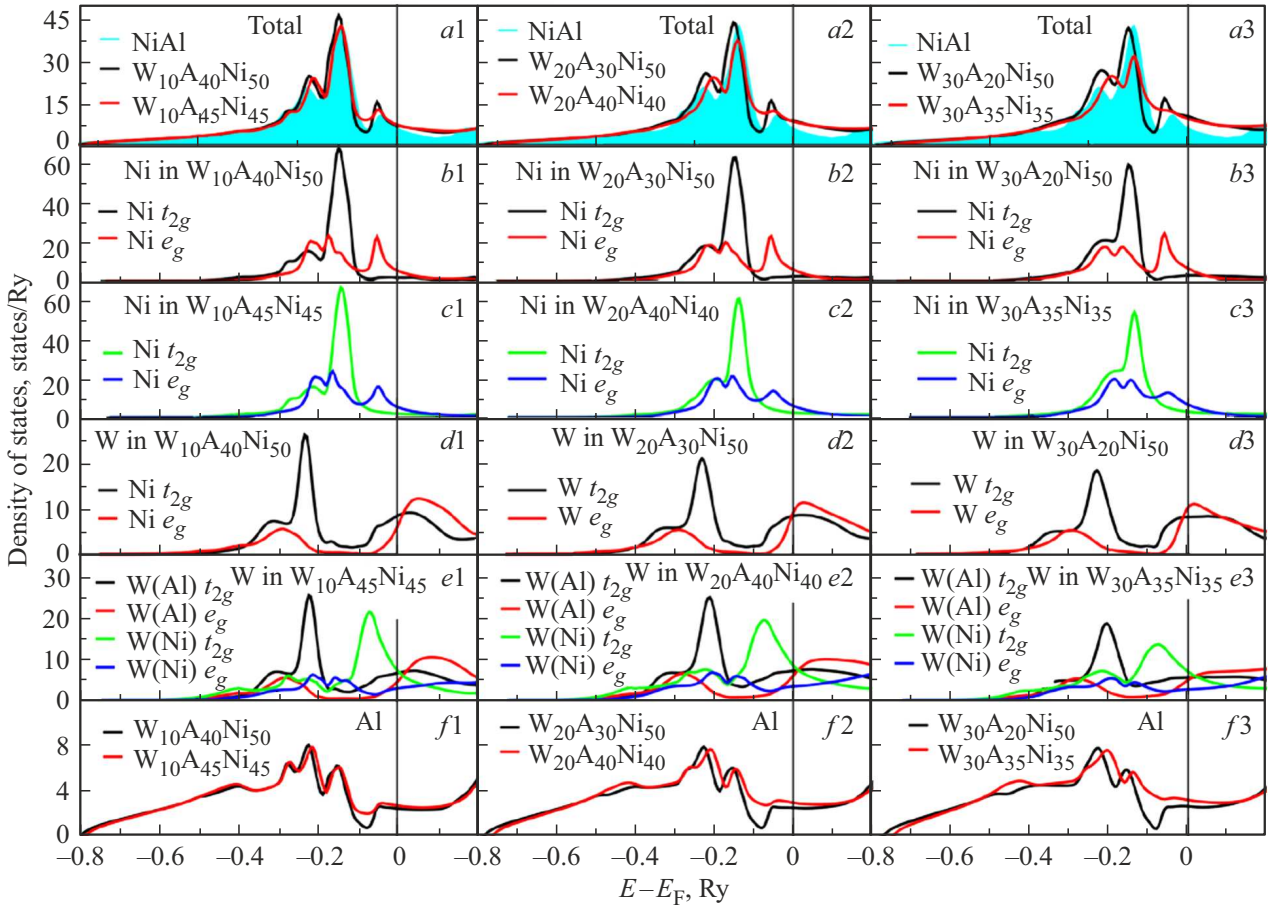

Figure 2. Total and partial density of electronic states (DOS) of $W_xAl_{50-x/2}Ni_{50-x/2}$ and $W_xAl_{50-x}Ni_{50}$ alloys.

to volume change compared to the shear resistance, and consequently, an increase in the volume modulus B and the constant C_{12} in alloys with a high-temperature distribution of tungsten. Indeed, as we have seen from Fig. 1, C_{12} and volume modulus B in $W_xAl_{50-x}Ni_{50}$ alloys vary more than in $W_xAl_{50-x/2}Ni_{50-x/2}$ alloys. The value of the constant $C_{11}W_xAl_{50-x}Ni_{50}$ of alloys in the concentration stability range varies slightly (Fig. 1), since the Nie_g states almost completely retain their shape (fig. 2, $b1-b3$). At the same time, the rapid growth of C_{12} with an increase in the concentration of W on the Al sublattice leads to the fact that the constant C' becomes negative at $x > 30$ and $W_xAl_{50-x}Ni_{50}$ alloys become mechanically unstable.

Thus, the appearance of t_{2g} tungsten electrons on the Ni sublattice leads to an increase in C_{44}, and e_g electrons W(Ni) — to increase C_{11} in alloys with low-temperature placement, i.e. placement of tungsten on the Ni sublattice increases mainly the covalent component of the atomic bond in $W_xAl_{50-x/2}Ni_{50-x/2}$ alloys. When placing tungsten on an aluminum sublattice, the interaction of W and Ni increases the uniformity of the electron density and strengthens the metallic component of the atomic bond in alloys of both types, but this effect is more pronounced in $W_xAl_{50-x}Ni_{50}$ alloys, since nickel it is not replaced by tungsten.

4. Conclusion

Using the method of exact MT orbitals in combination with the approximation of the coherent potential (EMTO-CPA) the effect of tungsten alloying on the elastic properties of B2-NiAl at low-temperature placement has been studied W on both sublattices and high temperature placement method W on the sublattice Al. It is shown that in $W_xAl_{50-x}Ni_{50}$ alloys with tungsten on the Al sublattice, there is a loss of mechanical stability and degradation of mechanical properties — a decrease in the elastic constant C_{44}, shear modulus G and Young's modulus E. However, at low concentrations of tungsten in the field of mechanical stability, a sharp increase in ductility is expected. At the same time, in $W_xAl_{50-x/2}Ni_{50-x/2}$ alloys with a low-temperature distribution of tungsten atoms, a rare combination of properties occurs — with an increase in the content of W, ductility increases and at the same time increases elastic constants C_{11} and C_{44}, shear modulus G and Young's modulus. The analysis of the density of electronic states showed that the simultaneous increase in

ductility and mechanical properties in $W_xAl_{50-x/2}Ni_{50-x/2}$ alloys is directly related to the change in the electronic structure during alloying.

Funding

The work was supported by the Russian Scientific Foundation (project No. 22−12-00193). The calculations were performed on the NITU computing cluster „MISiS".

Conflict of interest

The author declares that he has no conflict of interest.

References

[1] N. Trung, H. Phuong, M.D. Starostenkov. Lett. Mater. **9**, 168 (2019).
[2] E.M. Schulson, D.R. Barker. Scripta Met. **17**, 519 (1983).
[3] H. Li, J. Guo, H. Ye, Q. Wang, J.C. He. Mater. Lett. **62**, 61 (2008).
[4] G. Frommeyer, R. Rablbauer, H.J. Schafer. Intermetallics **18**, 299 (2010).
[5] K. Ishida, R. Kainuma, N. Ueno, T. Nishizawa. Met. Mater. Trans. A **22**, 441 (1991).
[6] V.V. Gostishchev, I.A Astapov, S.N. Khimukhin. Inorganic Mater.: Appl. Res. **8**, 546 (2017).
[7] E. Liu, Y. Gao, J. Jia, Y Bai, W. Wang. Mater. Sci. Eng. A **592**, 201 (2014).
[8] S. Ameri, Z Sadeghian, I Kazeminezhad. Intermetallics **76**, 41 (2016).
[9] A.I. Kovalev, D.L Wainstein, A.Y. Rashkovskiy. Appl. Surf. Sci. **354**, 323 (2015).
[10] C. Zhang, P. Han, J. Li, M. Chi, L. Yan, Y. Liu, X. Liu, B. Xu. J, Phys. D **41**, 095410 (2008).
[11] C. Jiang, J. Sordelet, B. Gleeson. Acta Mater. **54**, 2361 (2006).
[12] C. Zhang, F. Tian, X. Ni. Chin. Phys. B **29**, 036201 (2020).
[13] P. Lazar, R. Podloucky. Phys. Rev. B **73**, 104114 (2006).
[14] A.V. Ponomareva, E.I. Isaev, Yu.Kh. Vekilov, I.A. Abrikosov, Phys. Rev. B **85**, 144117 (2012).
[15] A.V. Ponomareva, Y.K. Vekilov, I.A. Abrikosov. J. Alloys Compd **586**, S274 (2014).
[16] K.P. Sidnov, D.S. Belov, A.V. Ponomareva, I.A. Abrikosov, A.M. Zharmukhambetova, N.V. Skripnyak, S.A. Barannikova, A.S. Rogachev, S. Rouvimov, A.S. Mukasyan. J. Alloys Compd. **688**, 534 (2016).
[17] C. Jiang. Acta Mater. **55**, 4799 (2007).
[18] L. Vitos. Computational Quantum Mechanics for Materials Engineers: The EMTO Method and Applications. Springer-Verlag, London (2007).
[19] G. Grimvall. Thermophysical Properties of Materials, 1st ed., Elsevier, N.Y. (1999).
[20] C. Asker, L. Vitos, I.A. Abrikosov. Phys. Rev. B **79**, 214112 (2009).
[21] D. Pettifor. Mater. Sci. Technol. **8**, 345 (1992).
[22] S.F. Pugh. Phil. Mag. **45**, 823 (1954).
[23] L. Vitos, I.A. Abrikosov, B. Johansson. Phys. Rev. Lett. **87**, 156401 (2001).
[24] L. Vitos, P.A. Korzhavyi, B. Johansson. Phys. Rev. Lett. **88**, 155501 (2002).
[25] J. Zhang, C. Cai, G. Kim, Y. Wang, W. Chen. npj Comput. Mater. **8**, 89 (2022).
[26] D. Music, T. Takahashi, L. Vitos, C. Asker, I.A. Abrikosov, J.M. Schneider. Appl. Phys. Lett. **91**, 191904 (2007).
[27] T. Gebhardt, D. Music, D. Kossmann, M. Ekholm, I.A. Abrikosov, L. Vitos, J.M. Schneider. Acta Mater. **59**, 3145 (2011).
[28] J. Zhang, P.A. Korzhavyi, J. He, Materials Today Commun. **28**, 102551 (2021).
[29] J.P. Perdew, K. Burke, M. Ernzerhof. Phys. Rev. Lett. **77**, 3865 (1996).
[30] J. Kollar, L. Vitos, H.L. Skriver. In: Electronic Structure and Physical Properties of Solids: The Uses of the LMTO Method, Lecture Notes in Physics / Ed. H. Dreysse. Springer-Verlag, Berlin (2000). P. 85.
[31] G. Simmons, H. Wang. Single Crystal Elastic Constants and Calculated Aggregate Properties: A Handbook. MIT Press, Cambridge, MA (1971).
[32] N. Rusovicand, H. Warlimont. Phys. Status Solidi A **44**, 609 (1977).
[33] T. Davenport, L. Zhou, J. Trivisonno Phys. Rev. B **59**, 3421 (1999)
[34] M. Mostoller, R. M. Nicklow, D. M. Zehner, S.-C. Lui, J.M. Mundenar, E.W. Plummer. Phys. Rev. B **40**, 2856 (1989).